Fatty acid amide hydrolase ablation promotes ectopic lipid storage and insulin resistance due to centrally mediated hypothyroidism

Whitney H. Brown[a,b,c], Matthew P. Gillum[a,b,c], Hui-Young Lee[a,b], Joao Paulo G. Camporez[b], Xian-man Zhang[b], Jin Kwon Jeong[d], Tiago C. Alves[b], Derek M. Erion[a,b,c], Blas A. Guigni[b], Mario Kahn[b], Varman T. Samuel[b], Benjamin F. Cravatt[e], Sabrina Diano[d], and Gerald I. Shulman[a,b,c,1]

[a]Howard Hughes Medical Institute and Departments of [b]Internal Medicine, [c]Cellular and Molecular Physiology, and [d]Ob/Gyn and Reproductive Sciences, Yale School of Medicine, New Haven, CT 06510; and [e]Department of Chemical Physiology, The Scripps Research Institute, La Jolla, CA 92037

Contributed by Gerald I. Shulman, July 26, 2012 (sent for review June 1, 2012)

Fatty acid amide hydrolase (FAAH) knockout mice are prone to excess energy storage and adiposity, whereas mutations in FAAH are associated with obesity in humans. However, the molecular mechanism by which FAAH affects energy expenditure (EE) remains unknown. Here we show that reduced energy expenditure in FAAH$^{-/-}$ mice could be attributed to decreased circulating triiodothyronine and thyroxine concentrations secondary to reduced mRNA expression of both pituitary thyroid-stimulating hormone and hypothalamic thyrotropin-releasing hormone. These reductions in the hypothalamic-pituitary-thyroid axis were associated with activation of hypothalamic peroxisome proliferating-activated receptor γ (PPARγ), and increased hypothalamic deiodinase 2 expression. Infusion of NAEs (anandamide and palmitoylethanolamide) recapitulated increases in PPARγ-mediated decreases in EE. FAAH$^{-/-}$ mice were also prone to diet-induced hepatic insulin resistance, which could be attributed to increased hepatic diacylglycerol content and protein kinase Cε activation. Our data indicate that FAAH deletion, and the resulting increases in NAEs, predispose mice to ectopic lipid storage and hepatic insulin resistance by promoting centrally mediated hypothyroidism.

T4 | T3 | TSH | diacylglycerols | ceramides

N-acylphosphatidylethanolamines (NAPEs) and *N*-acylethanolamines (NAEs) are nutrient-regulated lipokines that affect energy homeostasis through regulation of satiety and energy storage, selectively increasing in abundance with high-fat diet (HFD) feeding (1–7). NAPEs are hydrolyzed to produce diverse NAE species, which act as ligands for cannabinoid receptor 1 (CB1), G protein-coupled receptor 119 (GPR119), GPR55, peroxisome proliferating-activated receptor α (PPARα), and transient receptor potential cation channel subfamily V member 1 to affect appetite, gut hormone release, anxiety, and inflammation (8–12). Fatty acid amide hydrolase (FAAH) is the major enzyme responsible for the degradation of NAEs. An integral membrane protein, FAAH is expressed predominantly in the brain, liver, kidney, and intestine (13, 14). Mice lacking FAAH (FAAH$^{-/-}$ mice) have increased body weight after 12 wk of HFD feeding, independent of food intake (7) and decreased energy expenditure (EE) (15). Furthermore, SNPs in the *FAAH* gene correlate with obesity in humans (16, 17).

NAEs are lipid-signaling molecules that have diverse physiological effects. Anandamide (AEA), an endocannabinoid and an endogenous ligand of CB1, is the most well-studied NAE (11). Inhibition of CB1 promotes EE, leading to decreased body weight in HFD-fed mice (18). In addition, treatment with the CB1 inhibitor rimonabant increases oxygen consumption in isolated soleus muscle of obese mice (5).

Because FAAH is expressed in metabolically active tissues and may be a genetic cause of obesity in humans, we investigated EE and tissue-specific insulin sensitivity in FAAH$^{-/-}$ and FAAH$^{+/+}$ mice. To do so, we measured the expression of genes and hormones known to regulate EE, including PPARγ, proopiomelanocortin (POMC), and thyroid hormones. Here we show that FAAH regulates EE via the action of NAEs in the hypothalamus, leading to changes in PPARγ activation and alterations in the hypothalamic–thyroid axis in vivo.

Results

EE Is Decreased in Chow-Fed FAAH$^{-/-}$ Mice. In metabolic cage studies, EE was lower in 8-wk-old FAAH$^{-/-}$ mice compared with FAAH$^{+/+}$ mice (Fig. 1*A*). An ∼10% decrease in EE was observed during the light cycle when the mice were less active (Fig. 1*B*), in the absence of changes in locomotor activity (Fig. 1*C*). We next investigated the potential role of thyroid hormones in causing this reduction in whole-body EE and found ∼20–30% lower concentrations of plasma triiodothyronine (T_3) and thyroxine (T_4) in FAAH$^{-/-}$ mice compared with FAAH$^{+/+}$ mice ($P < 0.05$) (Fig. 1*D*).

The FAAH expression patterns led us to hypothesize that alterations in thyroid hormone signaling originate in the brain. Consistent with centrally mediated hypothyroidism, we found a 50% reduction in thyrotropin-releasing hormone (TRH) mRNA expression in the hypothalamus (Fig. 1*E*) and a 60% reduction in thyroid-stimulating hormone (TSH) mRNA expression in the pituitary gland (Fig. 1*F*). We also detected an 11-fold increase in hypothalamic deiodinase 2 (DIO2) mRNA expression (Fig. 1*G*). Because DIO2 is transcriptionally regulated by PPARγ, we investigated hypothalamic PPARγ activation in these mice. As we hypothesized, FAAH$^{-/-}$ mice exhibited increased hypothalamic PPARγ activation, as measured by the increased mRNA of PPARγ target genes, including glucokinase, glycerol kinase, perilipin, and CCAAT/enhancer-binding protein alpha (CEBPα) (19–22) (Fig. 1*H*).

PPARγ also regulates energy metabolism via the melanocortin system (23), and we observed suppression of hypothalamic POMC expression in FAAH$^{-/-}$ mice (Fig. 1*I*). Finally, treatment with the PPARγ inhibitor GW9662 increased EE in 12-wk-old FAAH$^{-/-}$ mice by 45%, rescuing the EE phenotype by increasing expenditure to FAAH$^{+/+}$ levels (Fig. 1*J*). CB1 inhibitors promote EE, leading to decreased body weight in vivo (18); thus, we postulated that increased activation of CB1 by anandamide

Author contributions: W.H.B., M.P.G., J.P.G.C., V.T.S., and G.I.S. designed research; W.H.B., M.P.G., H.-Y.L., J.P.G.C., X.Z., J.K.J., T.C.A., D.M.E., B.A.G., M.K., and S.D. performed research; B.F.C. contributed new reagents/analytic tools; W.H.B., M.P.G., H.-Y.L., J.P.G.C., X.Z., J.K.J., T.C.A., D.M.E., B.A.G., M.K., V.T.S., S.D., and G.I.S. analyzed data; and W.H.B., M.P.G., H.-Y.L., J.P.G.C., V.T.S., S.D., and G.I.S. wrote the paper.

The authors declare no conflict of interest.

Freely available online through the PNAS open access option.

[1]To whom correspondence should be addressed. E-mail: gerald.shulman@yale.edu.

This article contains supporting information online at www.pnas.org/lookup/suppl/doi:10.1073/pnas.1212887109/-/DCSupplemental.

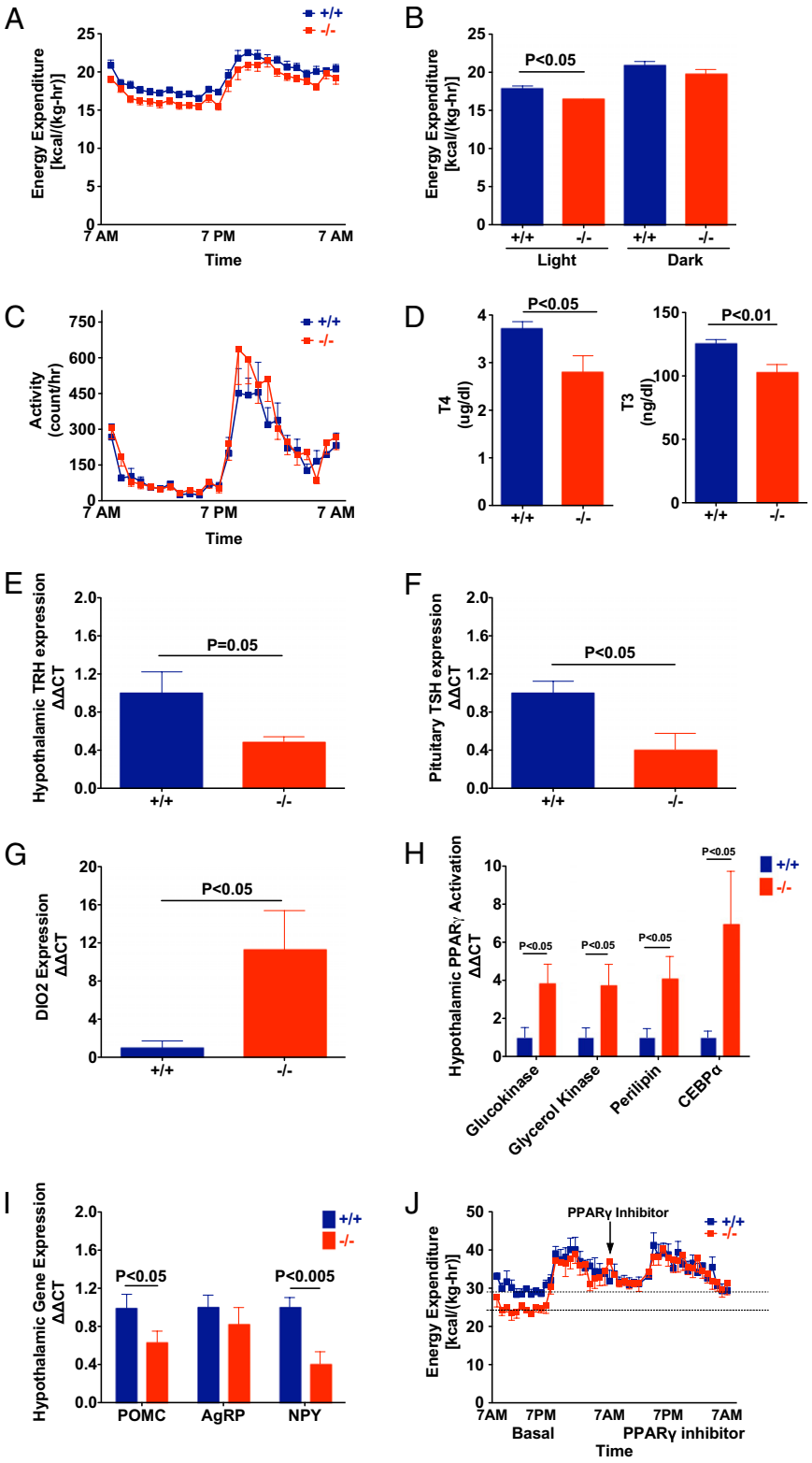

Fig. 1. Energy metabolism and downstream regulation. (*A*) EE was lower in 8-wk-old FAAH$^{-/-}$ mice compared with 8-wk-old FAAH$^{+/+}$ mice. (n = 12 per group), (*B*) Average EE was significantly lower during the light cycle, but not during the dark cycle, in FAAH$^{-/-}$ mice compared with FAAH$^{+/+}$ mice (n = 12 per group), (*C*) Locomotor activity during metabolic cage studies was similar in FAAH$^{-/-}$ mice and FAAH$^{+/+}$ mice. (n = 12 per group). (*D*) Plasma T_4 and T_3 concentrations were lower in FAAH$^{-/-}$ mice than in FAAH$^{+/+}$ mice (n = 5–6 per group). (*E*) Hypothalamic mRNA expression of TRH was lower in FAAH$^{-/-}$ mice compared with FAAH$^{+/+}$ mice (n = 8 per group). (*F*) Pituitary mRNA expression of TSH was lower in FAAH$^{-/-}$ mice than in FAAH$^{+/+}$ mice (n = 5 per group). (*G*) mRNA expression of DIO2 in hypothalamus was greater in FAAH$^{-/-}$ mice compared with FAAH$^{+/+}$ mice (n = 5–6 per group). (*H*) mRNA expression of PPARγ gene targets in the hypothalamus was greater in FAAH$^{-/-}$ mice than in FAAH$^{+/+}$ mice (n = 6–7 per group). (*I*) Hypothalamic mRNA expression of POMC (n = 20 per group), and neuropeptide Y (n = 8 per group) were lower in FAAH$^{-/-}$ mice compared with FAAH$^{+/+}$ mice, but that of Agouti-related peptide was similar in the two groups (n = 16 per group). (*J*) Inhibition of PPARγ activity with PPARγ agonist GW9662 restored EE to a greater degree in 12-wk-old FAAH$^{-/-}$ mice than in 12-wk-old FAAH$^{+/+}$ mice (n = 4 per group).

would be sufficient to decrease EE in FAAH$^{-/-}$ mice. Inhibition of CB1 by rimonabant was insufficient to rescue the FAAH$^{-/-}$ phenotype, however (Fig. S1). The EE phenotype was more pronounced in 12-wk-old chow-fed mice (Fig. 1 *A* and *J*).

NAEs Regulate EE. To directly examine whether increases in NAEs [palmitoylethanolamide (PEA) and AEA] were responsible for the reduced EE in FAAH$^{-/-}$ mice, we infused WT mice with PEA or AEA via mini osmotic pumps implanted s.c.. This treatment resulted in an ~50–100% increase in circulating concentrations of these metabolites, as well as a 20–200% increase in brain AEA and PEA concentrations, comparable to the differences seen in FAAH$^{-/-}$ and FAAH$^{+/+}$ mice (Fig. S2). The PEA and AEA infusions decreased EE by 15% and 10%,

respectively (Fig. 2 *A* and *D*). AEA has been shown to activate PPARγ in cultured adipocytes (24). Consistent with that finding, PEA and AEA infusions increased PPARγ activation in the hypothalamus, as reflected by increased expression of glucokinase, glycerol kinase, and CEBPα (Fig. 2 *B* and *E*). Furthermore, PEA and AEA infusion led to significant increases in hypothalamic DIO2 expression (Fig. 2 *C* and *F*). These results demonstrate that NAEs (PEA and AEA) have the capacity to activate hypothalamic PPARγ in vivo, resulting in decreased EE.

FAAH$^{-/-}$ Mice Are Prone to Hepatic Steatosis and Hepatic Insulin Resistance. To assess the effects of FAAH on glucose homeostasis, we fed FAAH$^{-/-}$ and FAAH$^{+/+}$ mice HFD for 4 wk and then measured whole-body glucose homeostasis by i.p. glucose tolerance tests (IPGTTs) and hyperinsulinemic-euglycemic (HE) clamp studies. For these studies, the mice were matched for body weight and fat mass (Fig. S3). By limiting high-fat feeding to 4 wk, we were able to study glucose metabolism before divergences in body weight occurred, as reported previously (7). FAAH$^{-/-}$ mice displayed mild glucose intolerance, as reflected by higher plasma glucose concentrations compared with WT mice during IPGTT (Fig. 3 *A* and *B*).

To further examine the mechanisms responsible for glucose intolerance in these mice, we performed HE clamping in combination with administration of radiolabeled glucose to assess insulin action in liver, muscle, and adipose tissue. FAAH$^{-/-}$ mice exhibited greater whole-body insulin resistance compared with FAAH$^{+/+}$ mice, as reflected by a 30% reduction in the glucose infusion rate required to maintain euglycemia during the HE clamp studies (Fig. 3 *C* and *D*) despite similar plasma insulin concentrations (Fig. 3*E*). The reductions in whole-body insulin sensitivity in the FAAH$^{-/-}$ mice could be attributed entirely to hepatic insulin resistance, as reflected by a higher rate of endogenous glucose production during the HE clamp study (Fig. 3*F*), resulting in a 45% suppression of glucose production in FAAH$^{-/-}$ mice, compared with a 90% suppression in FAAH$^{+/+}$ mice (Fig. 3*G*). In contrast, there was no difference in insulin-stimulated peripheral glucose uptake between the groups (Fig. 3*H*).

To investigate the mechanisms by which FAAH deletion decreases hepatic insulin sensitivity, we measured hepatic lipid content and found higher triglyceride and diacylglycerol (DAG) concentrations in FAAH$^{-/-}$ mice compared with FAAH$^{+/+}$ mice (Fig. 4 *A* and *B*). In contrast, we found no differences in liver ceramide content between the two groups (Fig. S4). This increase in hepatic DAG content was associated with a fourfold increase in protein kinase Cε (PKCε) activation, as reflected by increased translocation of PKCε to the plasma membrane (Fig. 4*C*), and impaired insulin-stimulated insulin receptor substrate 2 (IRS-2) tyrosine phosphorylation (Fig. 4*D*). Taken together, these data demonstrate that FAAH deletion promotes reductions in whole-body EE, predisposing FAAH$^{-/-}$ mice to ectopic lipid (DAG) accumulation in the liver and hepatic insulin resistance.

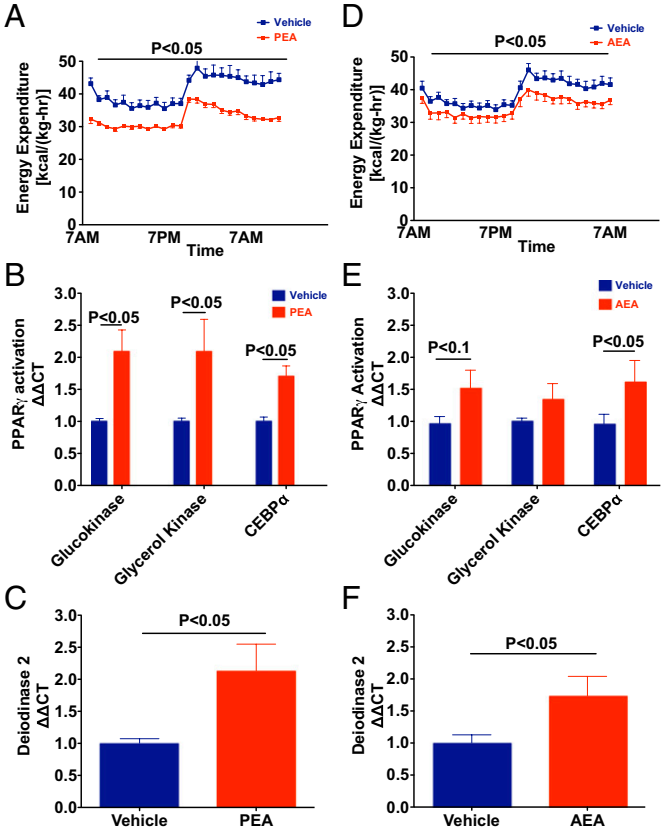

Fig. 2. Chronic s.c. infusions of NAEs (PEA and AEA) leads to decreased EE. (*A*) Chronic PEA infusion decreased EE by 18% compared with vehicle-treated mice. (*B*) PEA infusion led to hypothalamic PPARγ activation, as reflected by increased mRNA expression of glucokinase, glycerol kinase, and CCAAT/enhancer-binding protein α (CEBPα). (*C*) PEA infusion led to increased hypothalamic expression of DIO2. (*D*) AEA infusion decreased EE by 10% compared with vehicle-treated mice. (*E*) AEA infusion led to hypothalamic PPARγ activation, as reflected by increased mRNA expression of glucokinase, glycerol kinase, and CEBPα. (*F*) AEA infusion led to increased hypothalamic expression of DIO2 (Fig. S2).

Discussion

To date, FAAH has been studied mainly for its role in neurobiology. Based on its expression in organs central to metabolism, we hypothesized that FAAH might play a role in energy balance and glucose homeostasis. Here we describe a previously unreported role of FAAH as a central regulator of EE, and propose a mechanism by which elevated levels of NAEs may exacerbate diet-induced hepatic insulin resistance through the accumulation of ectopic lipids in the liver.

In this study, the FAAH$^{-/-}$ mice exhibited reduced whole-body EE, independent of activity. Given the key role of circulating thyroid hormones in the regulation of whole-body EE, we measured plasma concentrations of T_3 and T_4 and found 20–30% reductions in both hormones in FAAH$^{-/-}$ mice compared with FAAH$^{+/+}$ mice. To determine whether these reductions in plasma T_3 and T_4 concentrations were related to primary hypothyroidism or to central causes, we assessed the pituitary expression of TSH and hypothalamic expression of TRH. We found that expression of both TSH and TRH was decreased by >50% in FAAH$^{-/-}$ mice, implicating a hypothalamic-related cause of the hypothyroidism in these mice. Recent studies have demonstrated that increased hypothalamic expression of DIO2 results in local increases in T_3 that suppress TRH and TSH (25, 26), and that DIO2 expression is regulated by PPARγ activity (27). Moreover, AEA has been shown to increase PPARγ activity in cultured adipocytes (24).

Given that NAEs are substrates for FAAH, we hypothesized that ablation of FAAH would lead to increases in hypothalamic NAEs, resulting in activation of PPARγ, increased DIO2 expression in the hypothalamus, and centrally mediated hypothyroidism in FAAH$^{-/-}$ mice. Consistent with this hypothesis, we found that FAAH$^{-/-}$ mice exhibited increased hypothalamic PPARγ activity, as reflected by increased hypothalamic expression of PPARγ-responsive genes, including hypothalamic DIO2. These findings, along with reductions in whole-body EE, were recapitulated by chronic infusions of PEA and AEA in C57BL6 WT mice. Finally, pharmacologic inhibition of PPARγ with GW9662 restored the EE of FAAH$^{-/-}$ mice to WT levels. Although we observed no effect of CB1 inhibition on EE in the

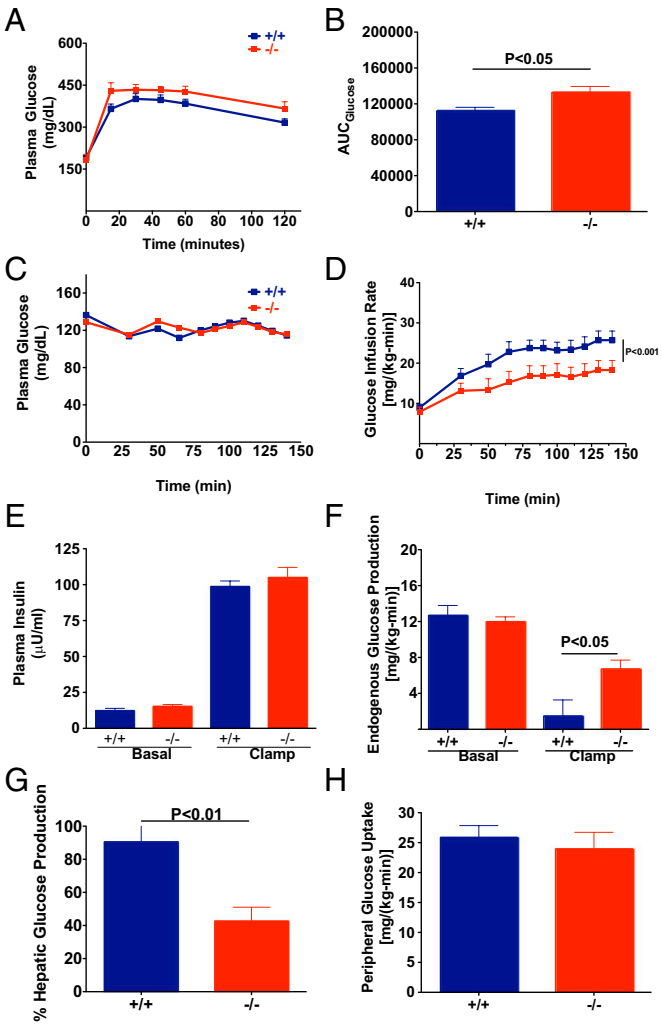

Fig. 3. FAAH$^{-/-}$ mice are prone to diet-induced hepatic steatosis and hepatic insulin resistance. (*A* and *B*) FAAH$^{-/-}$ mice manifested mild glucose intolerance during an IPGTT after an overnight fast (n = 5–8 per group). (*C*) Plasma glucose concentrations in FAAH$^{-/-}$ mice and FAAH$^{+/+}$mice during the HE clamp studies (n = 8–9 per group). (*D*) Glucose infusion rates required to maintain euglycemia during the HE clamp studies were lower in FAAH$^{-/-}$ mice than in FAAH$^{+/+}$ mice (n = 8–9 per group). (*E*) Plasma insulin concentrations were similar in the basal state and clamped state in FAAH$^{-/-}$ and FAAH$^{+/+}$mice (n = 8–9 per group). (*F*) Endogenous glucose production was similar in the two groups of mice in the basal state and increased in FAAH$^{-/-}$ mice during the HE clamp studies (n = 8–9 per group). (*G*) Suppression of endogenous glucose was more impaired in FAAH$^{-/-}$ mice compared with FAAH$^{+/+}$ mice during the HE clamp studies (n = 8–9 per group). (*H*) Insulin-stimulated peripheral glucose uptake was similar in FAAH$^{-/-}$ mice and FAAH$^{+/+}$ mice during the HE clamp studies (n = 8–9 per group) (Fig. S3).

FAAH$^{-/-}$ mice, it is possible that a sustained increase in hypothalamic AEA could lead to dysregulation of the CB1 receptor. Taken together, these data support our hypothesis that the decreased EE in FAAH$^{-/-}$ mice can be attributed, at least in part, to hypothalamic activation of PPARγ from increased levels of hypothalamic NAEs, which serve as endogenous ligands for PPARγ, resulting in increased hypothalamic expression of DIO2 and centrally mediated hypothyroidism. These findings are consistent with recent studies demonstrating that mice lacking PPARγ in neurons had increased EE and that administration of the PPARγ activator rosiglitazone in the brain led to significant increases in body weight (28). Along with the effect of PPARγ activation on the hypothalamic–thyroid axis, it is also possible that PPARγ mediates some of its effects to modify whole-body energy metabolism by altering the hypothalamic melanocortin axis, as reflected by reductions in hypothalamic POMC expression in FAAH$^{-/-}$ mice (23).

To evaluate the weight-independent effects of FAAH ablation on tissue-specific insulin sensitivity, we fed age- and weight-matched FAAH$^{-/-}$ and FAAH$^{+/+}$ mice a HFD for 4 wk and performed IPGTT and HE clamp studies before the occurrence of genotype divergence in weight or fat mass. We found that deletion of FAAH resulted in mild glucose intolerance associated with whole-body insulin resistance, as reflected by a 30% reduction in the glucose infusion rate required to maintain euglycemia during HE clamp studies. This whole-body insulin resistance could be entirely attributed to hepatic insulin resistance, as reflected by decreased suppression of endogenous glucose production during the HE clamp studies.

Previous studies in both rodents and humans have demonstrated that ectopic deposition of fat in liver associated with increases in hepatic DAG content and PKCε activation can lead to hepatic insulin resistance (29–31). Furthermore, knockdown of hepatic PKCε expression has been shown to protect rats from diet-induced hepatic insulin resistance (32). Consistent with this mechanism, we observed a 40% increase in hepatic DAG content in the FAAH$^{-/-}$ mice, associated with a marked increase in PKCε activation and a 60% reduction in insulin-stimulated IRS-2 tyrosine phosphorylation.

In summary, FAAH regulates the termination of endocannabinoid and related NAE signaling. By tuning the intricate balance of NAEs, both circulating and in tissues, FAAH is positioned to modulate a number of essential cellular processes. Known physiological functions of NAEs include the analgesic and anti-inflammatory effects of PEA (33) and the satiating effects of oleoylethanolamide (3). Expanding on these observations, we demonstrate the potential role of NAEs in promoting central

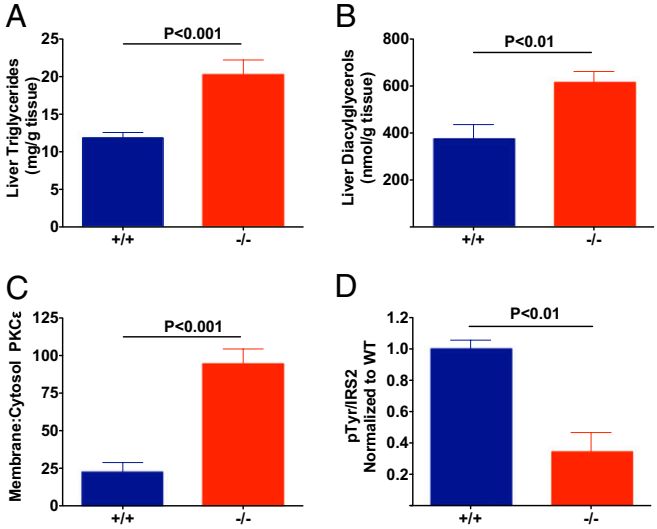

Fig. 4. FAAH$^{-/-}$ mice display increased hepatic triglyceride and DAG content associated with PKCε activation and reduced insulin-stimulated IRS-2 tyrosine phosphorylation on a HFD. (*A*) Liver triglyceride concentrations were higher in FAAH$^{-/-}$ mice compared with FAAH$^{+/+}$ mice after 4 wk of the HFD (n = 16 per group). (*B*) Hepatic DAG concentrations were higher in FAAH$^{-/-}$ mice compared with FAAH$^{+/+}$ mice as assessed by LC/MS/MS (n = 8 per group). (*C*) PKCε activity was higher in FAAH$^{-/-}$ mice compared with FAAH$^{+/+}$, as reflected by increased PKCε translocation from cytosol (c) to the plasma membrane (m) (n = 4 per group). (*D*) Insulin-stimulated IRS-2 tyrosine phosphorylation was lower in livers of FAAH$^{-/-}$ mice compared with FAAH$^{+/+}$ mice (n = 3–4 per group) (Fig. S3).

PPARγ activation, centrally mediated hypothyroidism, and decreased whole-body EE. This decrease in whole- body EE in turn predisposes $FAAH^{-/-}$ mice to ectopic lipid accumulation in the liver and hepatic insulin resistance. Our data elucidate a unique mechanism by which NAEs may regulate EE via the hypothalamic–pituitary–thyroid axis.

Methods

Animals. $FAAH^{+/+}$ and $FAAH^{-/-}$ mice were generated in the B.F.C. laboratory as described previously (34). Mice were maintained on a standard 12-h/12-h light–dark cycle in the Yale Animal Resources Center with ad libitum access to food pellets (2018S; Harlan Laboratories), and water unless indicated otherwise. All experiments were approved by the Yale University Animal Care and Use Committee.

LC/MS/MS Analyses. All LC/MS/MS analyses were performed on a benchtop ABI 4000 QTRAP LC/MS/MS system (Applied Biosystems) equipped with a Dionex UltiMate capillary liquid chromatograph and a Dionex Famos autosampler in conjunction with a PEAK Scientific gas generator, as described previously (1).

Basal Mouse Studies. Mice were housed under controlled temperature (22 ± 2 °C) and lighting (12-h light/12-h dark) with water and food provided ad libitum. $FAAH^{+/+}$ and $FAAH^{-/-}$ mice were fed a regular chow diet (TD2018; Harlan Teklad). To assess the effect of high-fat feeding on insulin action in $FAAH^{+/+}$ and $FAAH^{-/-}$ mice, an HFD (60% calories by fat; Research Diets D12492) was fed to the mice (age 5–6 wk) for 4 wk. Fat and lean body mass were assessed by ^{1}H NMR (Bruker BioSpin).

Metabolic Cage Experiments. Mice were allowed to acclimate to the calorimetric apparatus in individual cages. The Oxymax Comprehensive Minimal Metabolic Monitoring System (Columbus Instruments) was used to evaluate activity, food consumption, and EE. EE and respiratory quotient (RQ) were calculated from the gas-exchange data [$EE = (3.815 + 1.232 \times RQ) \times VO_2$], with RQ determined as the ratio of VCO_2 to VO_2. Activity was measured in both horizontal and vertical directions using infrared beams to count the beam breaks during the study. Feeding was measured by recording the difference in scale measurements of the center feeder from one time point to another. Drinking was assessed with a computerized system that counted water droplets consumed.

Receptor Inhibitor Studies. After a 24-h basal period and 2 h before the start of the light cycle, mice were given an i.p. Injection of GW9662 (1 mg/kg), rimonabant (10 mg/kg), or vehicle. Calorimetry studies were continued for 24 h after injection.

NAE Infusion in Metabolic Cages. A mini-osmotic pump (Alzet) containing PEA (10 mg/mL) or AEA (2 mg/mL) was implanted s.c. in each animal. NAEs were infused at a constant rate of 1 μL/h for 7 d. AEA infusions resulted in a twofold increase in plasma AEA concentrations, whereas PEA infusion achieved a 50% increase in plasma PEA concentrations (Fig. S2). The mice were killed after NAE administration, and plasma and hypothalami were collected for quantitative PCR (qPCR) and hormone measurements.

HE Clamp Studies. HE clamp studies were conducted as described previously (35, 36). Overnight-fasted mice were continuously infused with [3-^{3}H]glucose at 0.05 μCi/min over 2 h to assess basal rates of glucose turnover. After infusion of [3-^{3}H]glucose, HE clamp study was conducted for 140 min with a primed continuous infusion of insulin [Humulin, 21 mU/kg primed over 3 min, 3 mU/(kg-min) infusion rate; Novo Nordisk] and a variable infusion of 20% dextrose to maintain euglycemia (120 mg/dL). [3-^{3}H]glucose was infused continuously at 0.1 μCi/min to evaluate insulin-stimulated glucose uptake and endogenous glucose production. Samples were obtained at 0 and 135 min for evaluation of insulin concentrations. At study completion, mice were anesthetized, and tissues were harvested within 3 min with liquid N_2-cooled aluminum tongs and then stored at −80 °C for subsequent analysis.

Biochemical Analysis and Calculations. Plasma glucose concentrations were analyzed by the glucose oxidase method on a YSI 2700 Biochemistry Analyzer. Plasma insulin concentrations were measured using LINCO RIA kits (Millipore). Plasma [^{3}H]glucose was measured by scintillation counting of $ZnSO_4$/$Ba(OH)_2$ deproteinized serum, dried to remove $^{3}H_2O$. Endogenous glucose production rate was calculated as (rate of total glucose appearance) – (glucose infusion rate). Tissue DAG and ceramide extraction and analysis were performed as described previously (37).

Immunoblot Analysis. Membrane and cytosol of liver samples were separated by centrifugation and assayed for PKCε activation under basal conditions after a 6-h fast. Membrane and cytosolic proteins were separated by SDS/PAGE gel and transferred to nitrocellulose membranes. Antibodies against PKCε (Abcam) were used to determine protein abundance. PKCε found at the membrane was considered active. Blots were quantified using ImageJ analysis software (38). IRS-2 tyrosine phosphorylation was assessed after a 20-min insulin stimulation (3 mg/kg i.p.) in liver protein extracts. IRS-2 was immunoprecipitated using a polyclonal IRS-2 antibody (Cell Signaling) bound to protein A/G beads. Proteins were then run on an SDS/PAGE gel and blotted antibodies against p-tyrosine (Millipore) and monoclonal antibody against IRS-2 (Millipore) (38).

mRNA Quantification by qPCR. Hypothalamic total RNA was isolated using the RNeasy Kit (Invitrogen) and used in cDNA synthesis with a reverse-transcriptase kit (Qiagen). Then qPCR was performed as described previously (35) and normalized to β-actin. Primer sequences are displayed in Table S1.

Statistical Analysis. A two-tailed Student *t* test was used to test differences between $FAAH^{+/+}$ and $FAAH^{-/-}$ mice. Two-way ANOVA was performed to test multiple effects during the IPGTTs and HE clamp studies. Values are presented as mean ± SE; $P < 0.05$ was considered statistically significant.

ACKNOWLEDGMENTS. We thank the staff at the laboratory of Dr. Roy Weiss for their assistance with plasma T_3 and T_4 measurements. We also thank Debbie C. Jiang and Dr. Fitsum Guebre-Egziabher for their excellent technical support. This work was supported by US Public Health Service Grants F31 DK-083192, R01 DK-40936, R24 DK-085638, U24 DK-059635, R01 DK-084065, and P30 DK-45735 and a Mentor-Based Postdoctoral Award from the American Diabetes Association.

1. Gillum MP, et al. (2008) N-acylphosphatidylethanolamine, a gut-derived circulating factor induced by fat ingestion, inhibits food intake. *Cell* 135:813–824.
2. Kunz I, Meier MK, Bourson A, Fisseha M, Schilling W (2008) Effects of rimonabant, a cannabinoid CB1 receptor ligand, on energy expenditure in lean rats. *Int J Obes (Lond)* 32:863–870.
3. Rodríguez de Fonseca F, et al. (2001) An anorexic lipid mediator regulated by feeding. *Nature* 414:209–212.
4. Schwartz GJ, et al. (2008) The lipid messenger OEA links dietary fat intake to satiety. *Cell Metab* 8:281–288.
5. Liu YL, Connoley IP, Wilson CA, Stock MJ (2005) Effects of the cannabinoid CB1 receptor antagonist SR141716 on oxygen consumption and soleus muscle glucose uptake in Lep(ob)/Lep(ob) mice. *Int J Obes (Lond)* 29:183–187.
6. Osei-Hyiaman D, et al. (2008) Hepatic CB1 receptor is required for development of diet-induced steatosis, dyslipidemia, and insulin and leptin resistance in mice. *J Clin Invest* 118:3160–3169.
7. Touriño C, Oveisi F, Lockney J, Piomelli D, Maldonado R (2010) FAAH deficiency promotes energy storage and enhances the motivation for food. *Int J Obes (Lond)* 34:557–568.
8. Zygmunt PM, et al. (1999) Vanilloid receptors on sensory nerves mediate the vasodilator action of anandamide. *Nature* 400:452–457.
9. Fu J, et al. (2003) Oleylethanolamide regulates feeding and body weight through activation of the nuclear receptor PPAR-alpha. *Nature* 425:90–93.
10. Overton HA, et al. (2006) Deorphanization of a G protein-coupled receptor for oleoylethanolamide and its use in the discovery of small-molecule hypophagic agents. *Cell Metab* 3:167–175.
11. Devane WA, et al. (1992) Isolation and structure of a brain constituent that binds to the cannabinoid receptor. *Science* 258:1946–1949.
12. Ryberg E, et al. (2007) The orphan receptor GPR55 is a novel cannabinoid receptor. *Br J Pharmacol* 152:1092–1101.
13. Izzo AA, et al. (2001) Cannabinoid CB1-receptor mediated regulation of gastrointestinal motility in mice in a model of intestinal inflammation. *Br J Pharmacol* 134:563–570.
14. Cravatt BF, et al. (1996) Molecular characterization of an enzyme that degrades neuromodulatory fatty-acid amides. *Nature* 384:83–87.
15. Vaitheesvaran B, et al. (2012) Peripheral effects of FAAH deficiency on fuel and energy homeostasis: Role of dysregulated lysine acetylation. *PLoS ONE* 7:e33717.
16. Sipe JC, Waalen J, Gerber A, Beutler E (2005) Overweight and obesity associated with a missense polymorphism in fatty acid amide hydrolase (FAAH). *Int J Obes (Lond)* 29:755–759.
17. Monteleone P, et al. (2008) The cDNA 385C to A missense polymorphism of the endocannabinoid degrading enzyme fatty acid amide hydrolase (FAAH) is associated with overweight/obesity but not with binge eating disorder in overweight/obese women. *Psychoneuroendocrinology* 33:546–550.
18. Jbilo O, et al. (2005) The CB1 receptor antagonist rimonabant reverses the diet-induced obesity phenotype through the regulation of lipolysis and energy balance. *FASEB J* 19:1567–1569.
19. Guan HP, Ishizuka T, Chui PC, Lehrke M, Lazar MA (2005) Corepressors selectively control the transcriptional activity of PPARgamma in adipocytes. *Genes Dev* 19:453–461.

20. Arimura N, Horiba T, Imagawa M, Shimizu M, Sato R (2004) The peroxisome proliferator-activated receptor gamma regulates expression of the perilipin gene in adipocytes. *J Biol Chem* 279:10070–10076.
21. Kim SY, et al. (2004) Liver glucokinase can be activated by peroxisome proliferator-activated receptor-gamma. *Diabetes* 53(Suppl 1):S66–S70.
22. Rosen ED, et al. (2002) C/EBPalpha induces adipogenesis through PPARgamma: A unified pathway. *Genes Dev* 16:22–26.
23. Heaney AP, Fernando M, Yong WH, Melmed S (2002) Functional PPAR-gamma receptor is a novel therapeutic target for ACTH-secreting pituitary adenomas. *Nat Med* 8:1281–1287.
24. Bouaboula M, et al. (2005) Anandamide-induced PPARγ transcriptional activation and 3T3-L1 preadipocyte differentiation. *Eur J Pharm* 517:174–181.
25. Coppola A, et al. (2007) A central thermogenic-like mechanism in feeding regulation: An interplay between arcuate nucleus T3 and UCP2. *Cell Metab* 5:21–33.
26. Coppola A, Meli R, Diano S (2005) Inverse shift in circulating corticosterone and leptin levels elevates hypothalamic deiodinase type 2 in fasted rats. *Endocrinology* 146:2827–2833.
27. Grozovsky R, et al. (2009) Type 2 deiodinase expression is induced by peroxisomal proliferator-activated receptor-gamma agonists in skeletal myocytes. *Endocrinology* 150:1976–1983.
28. Ryan KK, et al. (2011) A role for central nervous system PPAR-γ in the regulation of energy balance. *Nat Med* 17:623–626.
29. Samuel VT, Petersen KF, Shulman GI (2010) Lipid-induced insulin resistance: Unravelling the mechanism. *Lancet* 375:2267–2277.
30. Kumashiro N, et al. (2011) Cellular mechanism of insulin resistance in nonalcoholic fatty liver disease. *Proc Natl Acad Sci USA* 108:16381–16385.
31. Samuel VT, Shulman GI (2012) Mechanisms for insulin resistance: Common threads and missing links. *Cell* 148:852–871.
32. Samuel VT, et al. (2007) Inhibition of protein kinase Cepsilon prevents hepatic insulin resistance in nonalcoholic fatty liver disease. *J Clin Invest* 117:739–745.
33. Re G, Barbero R, Miolo A, Di Marzo V (2007) Palmitoylethanolamide, endocannabinoids and related cannabimimetic compounds in protection against tissue inflammation and pain: Potential use in companion animals. *Vet J* 173:21–30.
34. Cravatt BF, et al. (2001) Supersensitivity to anandamide and enhanced endogenous cannabinoid signaling in mice lacking fatty acid amide hydrolase. *Proc Natl Acad Sci USA* 98:9371–9376.
35. Jurczak MJ, et al. (2012) Dissociation of inositol-requiring enzyme (IRE1α)-mediated c-Jun N-terminal kinase activation from hepatic insulin resistance in conditional X-box-binding protein-1 (XBP1) knock-out mice. *J Biol Chem* 287:2558–2567.
36. Jornayvaz FR, Shulman GI (2012) Diacylglycerol activation of protein kinase Cε and hepatic insulin resistance. *Cell Metab* 15:574–584.
37. Zhang D, et al. (2010) Resistance to high-fat diet-induced obesity and insulin resistance in mice with very long-chain acyl-CoA dehydrogenase deficiency. *Cell Metab* 11:402–411.
38. Samuel VT, et al. (2004) Mechanism of hepatic insulin resistance in non-alcoholic fatty liver disease. *J Biol Chem* 279:32345–32353.